

# A Novel Molecular Metal: (Oxamide oximato)(Oxamide oxime)nickel(II) Tetracyanoquinodimethanide, $[\text{Ni}(\text{oaoH})(\text{oaoH}_2)]\text{tcnq}$ , and Physical Properties of its Semiconducting Pt Analogue

Helmut Endres\*, August Bongart, Dietrich Nöthe

Anorganisch-Chemisches Institut der Universität,  
Im Neuenheimer Feld 270, D-6900 Heidelberg 1, FRG

Ingolf Hennig, Dieter Schweitzer

MPI für Medizinische Forschung, Abteilung Molekulare Physik,  
Jahnstr. 29 D-6900 Heidelberg 1, FRG

Herbert Schäfer\*\*, Hans W. Helberg

III. Physikalisches Institut der Universität, Bürgerstr. 42–44, D-3400 Göttingen, FRG

Serge Flandrois

Centre de Recherche Paul Pascal, Domaine Universitaire, F-33405 Talence, France

Z. Naturforsch. **40b**, 489–495 (1985); eingegangen am 15. November 1984

Molecular Metal, Radical Salt, Electronic Properties, Stacked Structure

$[\text{C}_4\text{H}_{11}\text{N}_8\text{NiO}_4]^+[\text{C}_{12}\text{H}_4\text{N}_4]^-$ ,  $M_r = 498.09$  is triclinic,  $P\bar{1}$ ,  $a = 3.7718(6)$ ,  $b = 7.436(2)$ ,  $c = 17.511(4)$  Å,  $\alpha = 88.67(2)$ ,  $\beta = 86.93(2)$ ,  $\gamma = 85.05(2)^\circ$ ,  $V = 488.51$  Å<sup>3</sup>,  $Z = 1$ ,  $d_c = 1.69$  gcm<sup>-3</sup>, final  $R_w = 0.035$  for 1454 observed independent reflections. The crystals consist of segregated regular parallel stacks of planar metal complex cations and  $\text{tcnq}^-$  counterions with intermolecular H bonds stabilizing the structure. The compound is metallic at room temperature. A metal to semiconductor transition around 230 K shows up in thermopower data, in the microwave conductivity and epr around 170 K. It is not visible in the static magnetic susceptibility.

## Introduction

The radical anion of tetracyanoquinodimethane ("tcnq", 2,2'-(2,5-cyclohexadiene-1,4-diyliidene)bispropanedinitrile) is a well-known component of organic metals [1]. These compounds consist of segregated stacks of tcnq and planar organic donor molecules [2], and a fractional average charge per tcnq unit seems to be a prerequisite for metallic behaviour [3]. Until now all attempts to prepare compounds of this type, with the organic donor replaced by a planar transition metal complex, had failed; there are only a few bis(arene)metal tcnq salts where segregated parallel stacks of cations and anions occur [4].

We expected that this kind of stacking could be stabilized by intermolecular H bridges. The metal complexes of oxamide oxime ("diaminoglyoxime",  $\text{oaoH}_2$ ,  $\text{HON}=\text{C}(\text{NH}_2)-\text{C}(\text{NH}_2)=\text{NOH}$ ) seemed suitable for this, as the amino groups may act as H

bridge donors. Furthermore, our experience with these complexes containing the metals Ni(II), Pd(II), Pt(II) showed, that they may be crystallized with different positive charges, as the degree of protolysis of the oxime groups depends on the pH during crystallization [5]. Thus, starting from  $[\text{Pt}(\text{oaoH}_2)_2]\text{Cl}_2$  and  $\text{Li}(\text{tcnq})$ , we obtained the salt  $[\text{Pt}(\text{oaoH})(\text{oaoH}_2)]\text{tcnq}$ , which was the first example of segregated regular stacks in a salt of a planar metal complex cation with an organic acceptor [6]. Physical measurements, reported below, revealed its semiconducting properties.

An analogous starting compound  $[\text{M}(\text{oaoH}_2)_2]\text{Cl}_2$  with  $\text{M} = \text{Ni}$  does not exist, as the reaction of  $\text{Ni}(\text{oaoH})_2$  with HCl normally affords  $[\text{Ni}(\text{oaoH}_2)_3]\text{Cl}_2$  [7] and in rare cases  $[\text{Ni}(\text{oaoH}_2)_2]\text{Cl}_2$  [8], both with a sixfold coordination of Ni(II). These complexes yield neutral  $\text{Ni}(\text{oaoH})_2$  when treated with a base, but the addition of ethanol to an aqueous solution of  $[\text{Ni}(\text{oaoH}_2)_3]\text{Cl}_2$  causes the crystallization of  $[\text{Ni}(\text{oaoH})(\text{oaoH}_2)]\text{Cl}$  with a planar monocationic complex cation [5]. This observation led us to the synthesis of  $[\text{Ni}(\text{oaoH})(\text{oaoH}_2)]\text{tcnq}$ , the structure and physical properties of which are described below.

\* Reprint requests to Prof. Dr. Helmut Endres.

\*\* New address: Siemens AG, Zentralbereich Technik, D-8000 München.

Verlag der Zeitschrift für Naturforschung, D-7400 Tübingen  
0340-5087/85/0400-0489/\$ 01.00/0

## Experimental

[Ni(oaoH)(oaoH<sub>2</sub>)]tcnq is obtained as a microcrystalline blue-black powder when an alcoholic solution of Li(tcncq) is added dropwise at room temperature to a stirred aqueous solution of [Ni(oaoH<sub>2</sub>)<sub>3</sub>]Cl<sub>2</sub>. Thin needle-like crystals of about 1 mm length can be grown by a diffusion method using a two-compartment cell with a sintered glass filter frit (G 4): One compartment is filled with a concentrated aqueous solution of the Ni complex salt, the other one with a concentrated methanolic solution of Li(tcncq). The crystals of the title compound form in the course of a few days in the compartment containing the Li(tcncq). They decompose around 280 °C and show  $\text{C}\equiv\text{N}$  stretching vibration as a doublet at 2165 and 2200  $\text{cm}^{-1}$ .

The dc-conductivity was measured by the standard four-probe method with dc and standard lock-in techniques at 4 Hz along the needle axis. The samples were mounted on gold wires in a teflon block. The contacts were made with silver paint and had a resistance of a few ohms. Both dc and lock-in methods gave identical results. Thermopower measurements were carried out in a device similar to that described by Chaikin and Kwak [9]. The Raman spectrum was taken at 1.3 K with the apparatus described earlier [10].

Static magnetic susceptibility measurements were performed on polycrystalline samples from 3 to 300 K by the Faraday method in fields up to 13.5 kG. Measurements at several values of the magnetic field did not show any ferromagnetic contamination of the samples. The paramagnetism was obtained from the measured values in the usual way by subtracting the core diamagnetism estimated to  $-2.30 \cdot 10^{-4}$  emu/mole from Pascal constants.

The microwave conductivity  $\sigma = 2\pi f \epsilon_0 \epsilon''$  ( $f$  frequency,  $\epsilon_0 = 8.854 \cdot 10^{-12}$  As/Vm dielectric constant of free space,  $\epsilon''$  imaginary part of the complex dielectric constant  $\epsilon = \epsilon' - i\epsilon''$ ) was measured in the temperature range from 10 to 300 K at 10.2 GHz using cavity perturbation technique (e.g. [11]). The frequency generator was controlled by the resonance frequency of the cavity in a feedback loop (frequency accuracy  $\approx 10^{-7}$ ). The cylindrical cavity (quality 8800) operates in the TE<sub>111</sub> mode. The single crystals were positioned into the maximum of the electric field inside the cavity with the needle axis parallel to the field.  $\sigma$  is calculated from the relative change in quality and the normalized frequency shift.

Epr measurements of a polycrystalline sample were performed on a Bruker B-ER 418 spectrometer equipped with a Bruker NMR gaussmeter for field calibration and an EIP 351 D microwave frequency

meter. Relative epr intensities were obtained by electronical double integration of the first derivative epr signal or by taking  $h \cdot H_{pp}^2$  ( $h$  = peak height,  $H_{pp}$  = peak-to-peak line width) as a measure for the epr intensity.

For the X-ray investigations a prismatic trunc of a crystal,  $0.05 \times 0.09 \times 0.14$  mm, was mounted on top of a glass capillary. Lattice parameters were derived from the setting angles of 25 reflections (Syntex R3 diffractometer, monochromated MoK $\alpha$  radiation). Data collection ( $\theta$ - $2\theta$  scans background-peak-background,  $2\theta < 58^\circ$ ) was carried out over the whole sphere of reciprocal space. An empirical absorption correction ( $\mu = 10.5 \text{ cm}^{-1}$ ) was applied using  $\psi$ -scans of 8 reflections. Equivalent reflections were averaged (merging  $R = 0.032$ ) to a set of 1454 observed independent reflections with  $I > 2\sigma(I)$ .

As the lattice constants were close to that of the Pt compound [6], its atom coordinates were taken as starting values. Refinement by cascade matrix least squares based on  $F$  with weights  $w = 1/\sigma^2(F)$  converged with  $R_w(R) = 0.035$  (0.043), a goodness of fit of 1.3 and a mean (max.) shift/error of .001 (0.003). H positions from a difference Fourier map were refined with individual isotropic temperature factors, the other atoms with anisotropic ones. Largest features in a final difference Fourier map were +0.55 and -0.36 electrons per  $\text{\AA}^3$ . For the discussion of the structure it is important that it could not be refined in the acentric space group P1.

Calculations were performed with the SHELXTL program package [12] on a Nova 3 computer using scattering factors, including anomalous dispersion, from International Tables for X-ray Crystallography [13]. Plots were done on a Tektronix plotter with SHELXTL.

## Results and Discussion

Atom coordinates are listed in Table I\*. The molecular ions with bond distances and angles are shown in Figs. 1 and 2, a stereoview of the structure in Fig. 3. The midpoints of both constituents lie on crystallographic inversion centers, and the H(6) atom of the cation is disordered over two equivalent sites. This contrasts the structure of the cation in [Ni(oaoH)(oaoH<sub>2</sub>)]Cl · H<sub>2</sub>O [5], which is acentric.

\* Lists of anisotropic temperature factors and observed and calculated structure factors have been deposited with the Fachinformationszentrum Energie, Physik, Mathematik, D-7514 Eggenstein-Leopoldshafen 2, FRG. Copies may be obtained quoting the deposition number CSD 51218, the authors, and the journal reference.

Table I. Atom coordinates ( $\times 10^4$ , H coordinates  $\times 10^3$ ) and isotropic temperature factors ( $\text{\AA}^2 \times 10^3$ ). For non-H atoms the equivalent values defined as 1/3 of the trace of the orthogonalized  $U_{ij}$  tensor are given.

Atom	x	y	z	U
Ni	0	10000	0	24(1)
N(1)	-1349(7)	10371(4)	1033(2)	28(1)
N(2)	-1864(7)	7797(4)	215(2)	29(1)
N(3)	-4036(9)	9136(5)	2129(2)	37(1)
N(4)	-4499(9)	6011(4)	1162(2)	38(1)
O(1)	-999(7)	11881(3)	1457(1)	41(1)
O(2)	-1906(8)	6401(4)	-289(1)	38(1)
C(1)	-2847(8)	9090(4)	1400(2)	24(1)
C(2)	-3140(9)	7517(4)	909(2)	25(1)
N(5)	1873(9)	5672(4)	2696(2)	48(1)
N(6)	1672(10)	286(4)	3657(2)	61(1)
C(3)	-3977(9)	6179(4)	4416(2)	28(1)
C(4)	-2738(8)	4314(4)	4379(2)	25(1)
C(5)	-3872(9)	3164(4)	4994(2)	28(1)
C(6)	-449(9)	3646(4)	3771(2)	29(1)
C(7)	807(9)	4778(5)	3176(2)	32(1)
C(8)	727(9)	1782(5)	3717(2)	36(1)
H(1)	0(10)	1264(5)	110(2)	66(14)
H(2)	-372(10)	1021(6)	242(2)	66(13)
H(3)	-502(8)	836(4)	233(2)	23(10)
H(4)	-508(11)	595(6)	163(2)	74(15)
H(5)	-488(9)	508(5)	82(2)	38(10)
H(6)	-96(23)	549(11)	-10(6)	62(30)
H(7)	-312(7)	191(4)	496(2)	27(8)
H(8)	-325(6)	692(3)	401(1)	11(7)

The complex is planar, with a max. deviation of a non-H atom from the least squares plane of 0.02(1)  $\text{\AA}$ . The cations form stacks along  $a$  with an interplanar spacing of 3.34(1)  $\text{\AA}$ . As usual, the  $\text{tcnq}^-$  anion is not exactly planar, and there is a dihedral

angle of 2.6(5) $^\circ$  between the planes through the ring and through the terminal  $(\text{CN})_2\text{C}$ -groups, respectively. The anions form regular stacks along  $a$  as well, with an interplanar spacing of 3.20(1)  $\text{\AA}$  between the ring planes. The overlap (Fig. 4) is of the type ring-external double bond, as often found in  $\text{tcnq}$  stacks. The angle between the ring plane of  $\text{tcnq}^-$  and the plane through the cation is 35.8(5) $^\circ$ , as in the Pt compound [6]. This is also true for the tilt angles of the molecular planes with respect to the  $a$  axis, 27.6(5) $^\circ$  for the complex cation and 32.0(5) $^\circ$  for  $\text{tcnq}^-$ .

As the precision of the structure determination is higher for the Ni compound than for the Pt counterpart and as all the H position could be determined, the H-bonding network which stabilizes the structure is much clearer (Fig. 5). The metal complex stacks are linked to sheets via intermolecular H bonds between the oxime groups involving the disordered H(6). This intermolecular bridge is weaker (2.642(5)  $\text{\AA}$ ) in the Ni salt than in the Pt salt (2.55(2)  $\text{\AA}$ ). On the other hand, the intramolecular H bridge between oxime O atoms is shorter (2.626(5)  $\text{\AA}$ ) in the Ni complex than in the Pt compound, 2.84(1)  $\text{\AA}$ , as a consequence of the smaller radius of Ni. A further H bridge connects the oxime O(2) with an amino group of the adjacent cation (Fig. 5). Cations and anions are linked by H bridges from the amino groups to the nitrile N atoms.

D.c. conductivity along the stacking axis (needle axis of the crystals) and thermopower measurements (Figs. 6, 7) revealed semiconducting behaviour in the Pt complex salt. According to epr intensity meas-

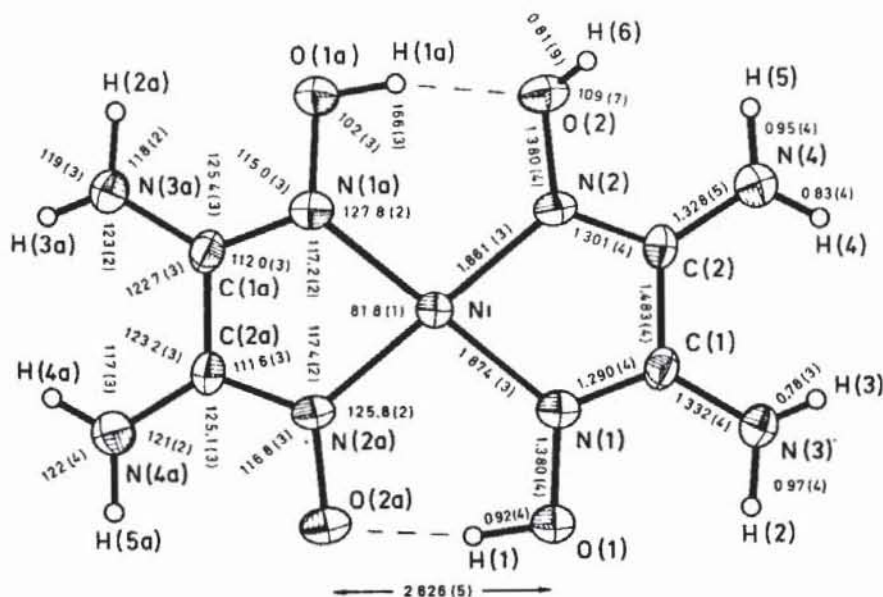


Fig. 1. The  $[\text{Ni}(\text{oaoH})(\text{oaoH}_2)]^+$  complex cation with bond distances and angles. Thermal ellipsoids are at the 50% probability level. H atoms are drawn as spheres with arbitrary radius.

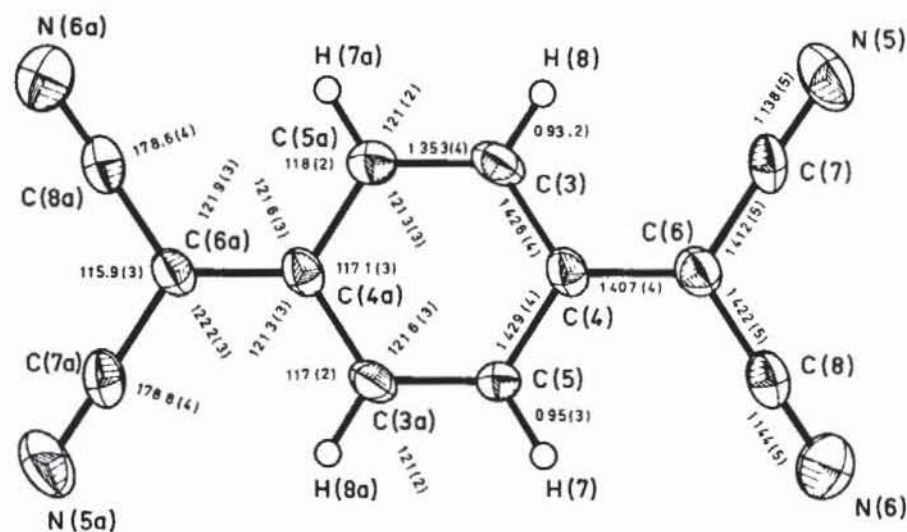


Fig. 2. The  $\text{tcnq}^-$  anion, analogous to Fig. 1.

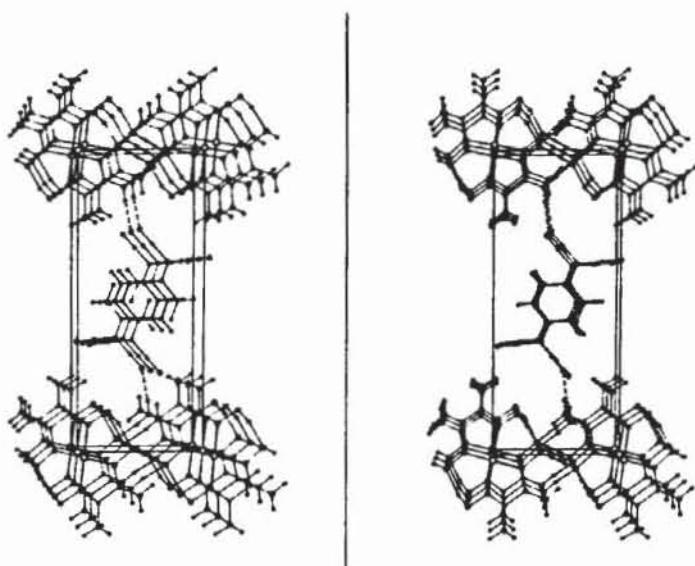


Fig. 3. Stereoview of the structure seen from a direction inclined at  $5^\circ$  to the  $a$ -axis.

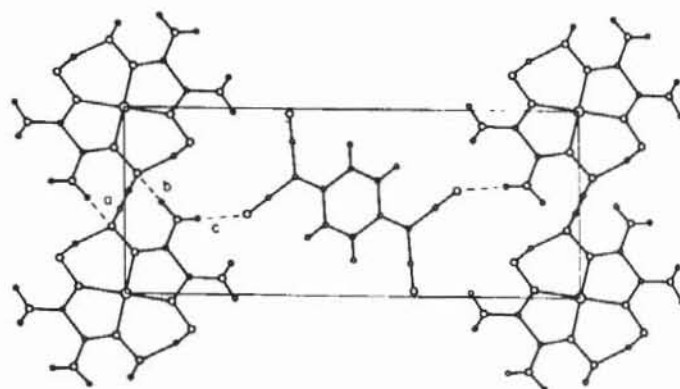


Fig. 5. Projection of the structure along  $a$ , indicating prominent intermolecular H bonds. Parameters are: a)  $\text{O}(2)\text{--O}(2a)$  2.642(5) Å,  $\text{H}(6)\text{--O}(2a)$  1.84(9) Å,  $\text{O}(2)\text{--H}(6)\text{--O}(2a)$   $170(8)^\circ$ ; b)  $\text{O}(2)\text{--N}(4a)$  2.857(5) Å,  $\text{O}(2)\text{--H}(5a)$  1.99(4) Å,  $\text{O}(2)\text{--H}(5a)\text{--N}(4a)$   $151(5)^\circ$ ; c)  $\text{N}(4a)\text{--N}(5)$  2.964(5) Å,  $\text{H}(4a)\text{--N}(5)$  2.16(5) Å,  $\text{N}(4a)\text{--H}(4a)\text{--N}(5)$   $163(5)^\circ$ .

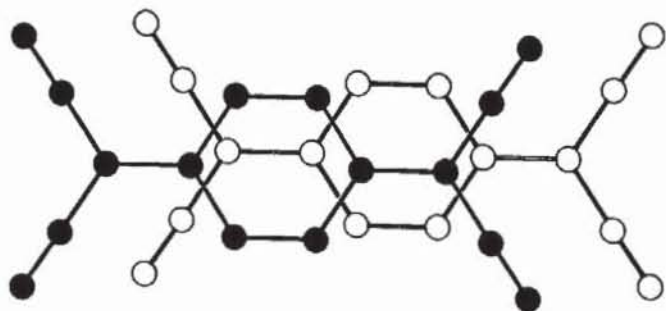


Fig. 4. Overlap pattern of two adjacent  $\text{tcnq}^-$  anions within a stack.

urements the paramagnetism increases with temperature between 100 and 400 K, *i.e.* the compound shows an activated paramagnetism. This physical behaviour is normal for a salt containing regular stacks of  $\text{tcnq}^-$  ions with integral charge [1–4].

The Ni compound, however, seems to be metallic at room temperature (Figs. 8–10): The d.c. conductivity shows a plateau at room temperature, and semiconductivity below  $\sim 250$  K. The thermopower exhibits a phase transition around 230 K, and the behaviour above this transition looks metal like: The small absolute value and the linear temperature dependence of the thermopower above the phase tran-

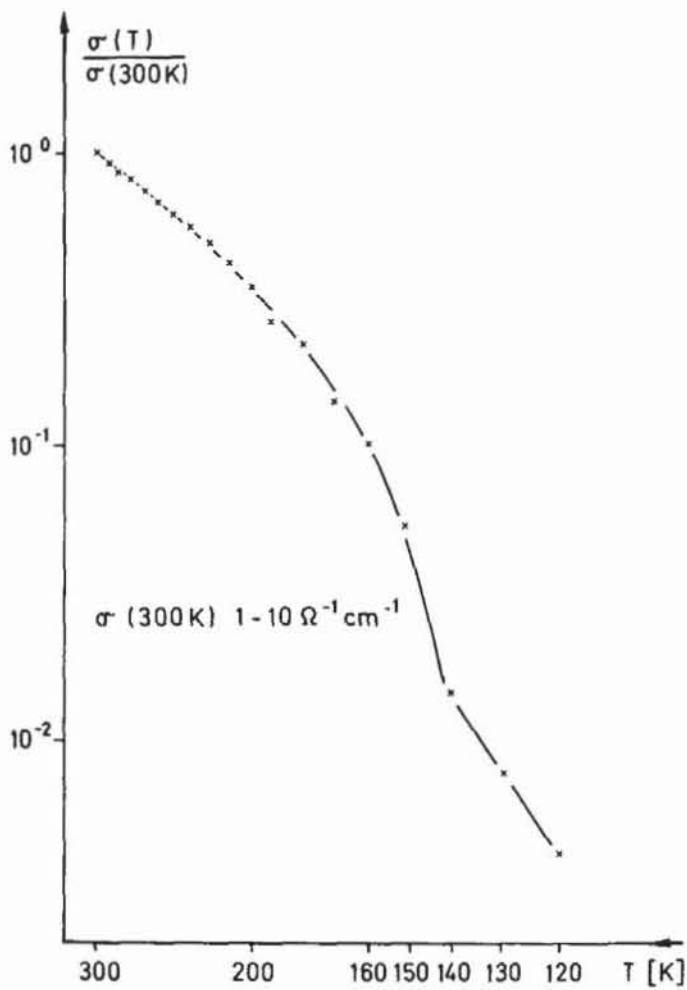


Fig. 6. Normalized d.c. conductivity of  $[\text{Pt}(\text{oaoH})(\text{oaoH}_2)]\text{tcnq}$  as a function of temperature.

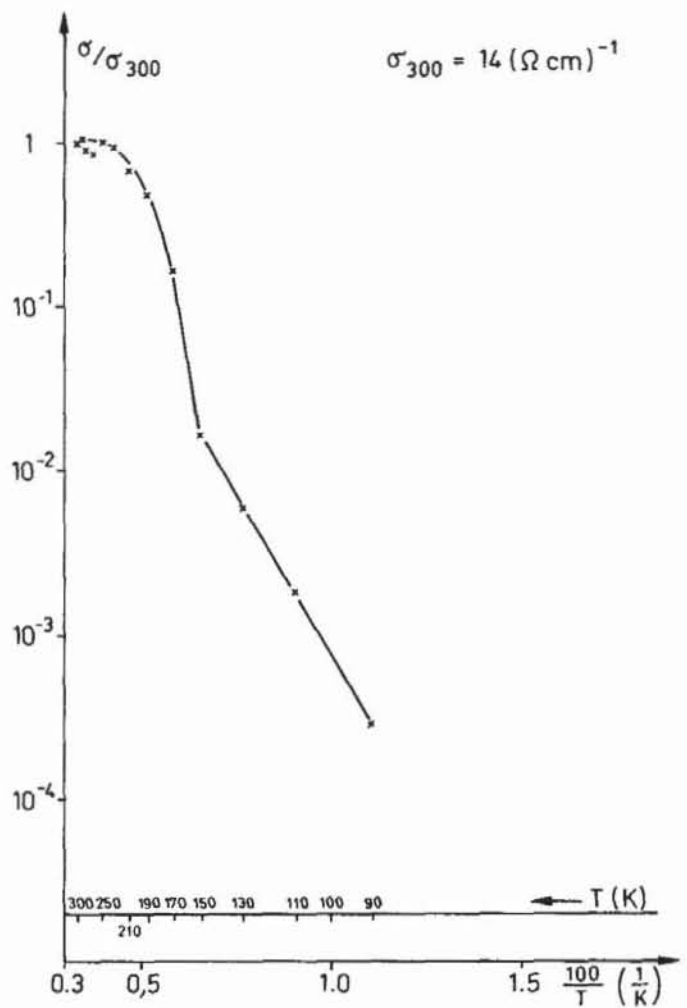


Fig. 8. Normalized d.c. conductivity of  $[\text{Ni}(\text{oaoH})(\text{oaoH}_2)]\text{tcnq}$ .

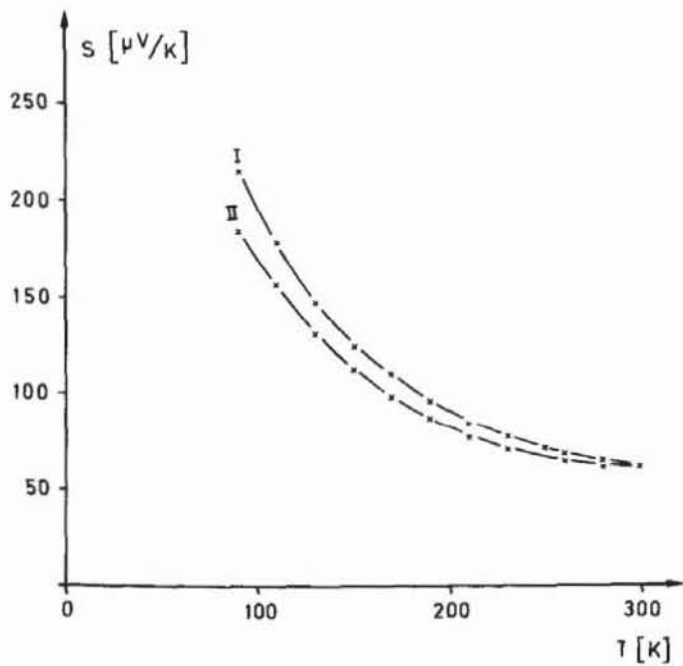


Fig. 7. Temperature dependence of the thermopower of two crystals of  $[\text{Pt}(\text{oaoH})(\text{oaoH}_2)]\text{tcnq}$ .

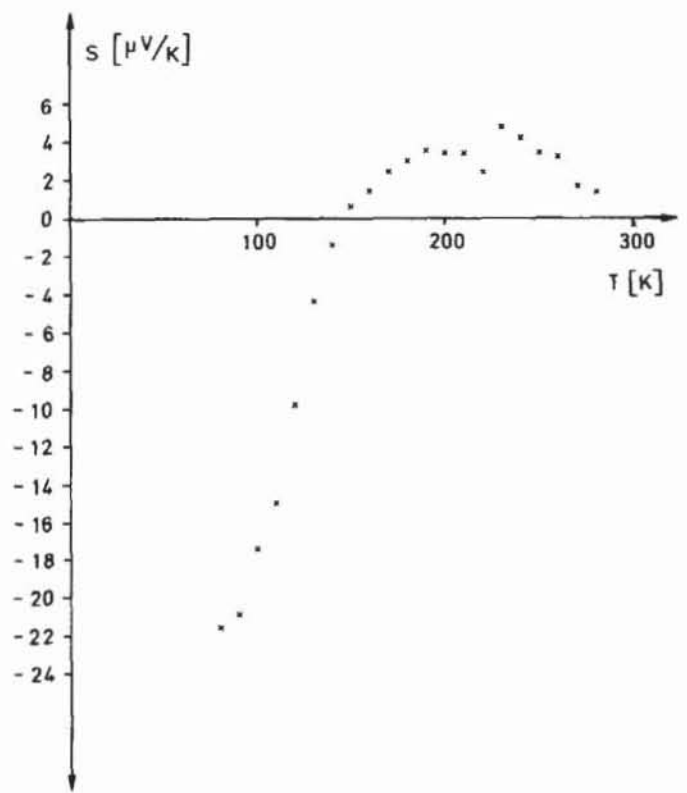


Fig. 9. Temperature dependence of the thermopower of  $[\text{Ni}(\text{oaoH})(\text{oaoH}_2)]\text{tcnq}$ .

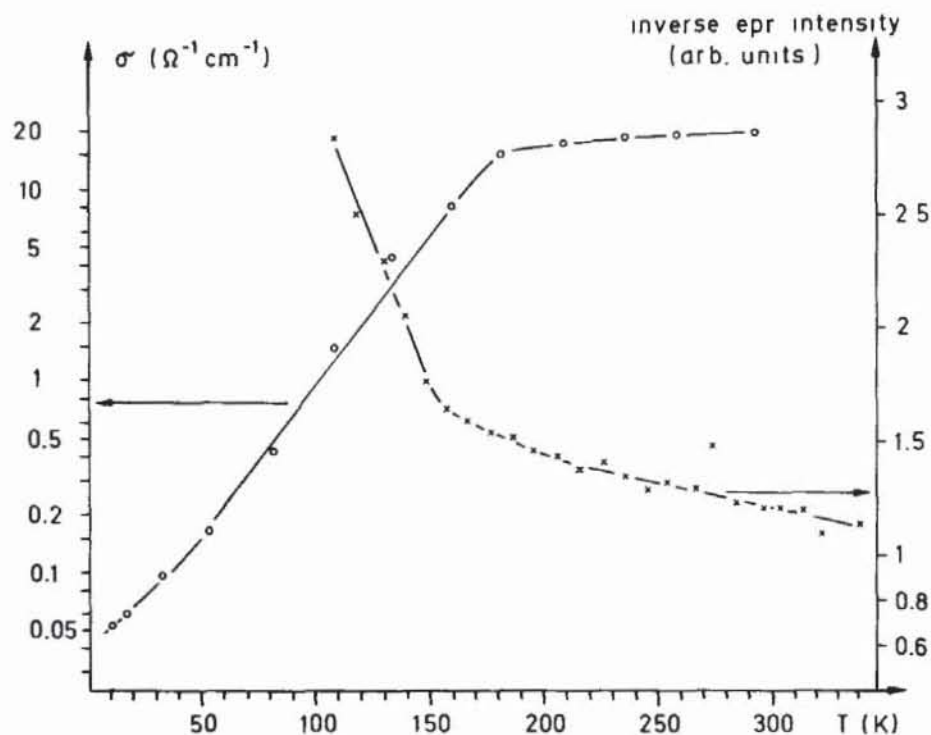


Fig. 10.  $[\text{Ni}(\text{oaoH})(\text{oaoH}_2)]\text{tcnq}$ : Temperature dependence of the microwave conductivity (circles, left scale) and of the inverse epr signal intensity (crosses, right scale). The solid lines are guides for the eye.

sition are reminiscent of a one-dimensional metal [14]; that the line does not extrapolate to zero at 0 K may be attributed to the contribution of a positive charge carrier to the total thermopower. This shifts the thermopower to positive values.

The epr signal intensity, Fig. 10, is only slightly temperature dependent, increasing roughly by 50% in going from 160 K to 360 K.

Below about 160 K the epr intensity is thermally activated and decreases strongly with decreasing temperature. This points at a spin pairing between adjacent  $\text{tcnq}^-$  species.

The conductivity measured by the microwave method is included in Fig. 10. Its room temperature value,  $20 \Omega^{-1}\text{cm}^{-1}$ , is in good agreement with d.c. measurements. However, it remains nearly constant down to  $\sim 170$  K when it switches to an activated conductivity. Thus, while thermopower data indicate a phase transition around 230 K, in agreement with dc conductivity, microwave conductivity and epr hint at a phase transition around 160–170 K. The reason behind this is not yet understood. (X-ray powder patterns by the Guinier technique do not reveal a structural change down to 160 K.)

No anomaly at all can be seen in the static magnetic susceptibility of a polycrystalline sample. (Fig. 11): The paramagnetism decreases slightly down to about 100 K. At low temperatures there is an increase and a small peak at 30 K which is prob-

ably due to  $\text{O}_2$  chemisorption. There are other examples of organic metals, *e.g.* some tetramethyltetra-thiafulvalene (tmttf) salts [15], which undergo a metal-to-insulator transition without any anomaly in the static magnetic susceptibility.

Now the difference of the physical properties of the isostructural Ni and Pt compounds remains to be explained. We suggest that the high temperature

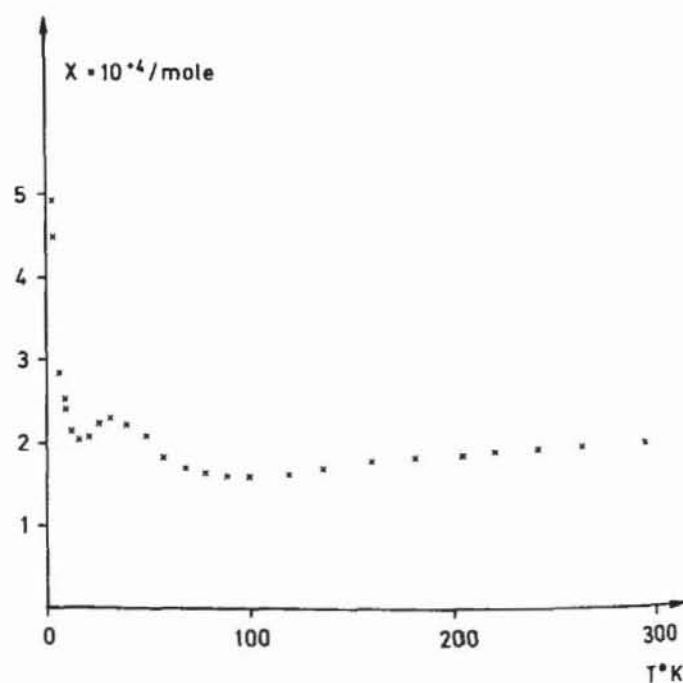


Fig. 11.  $[\text{Ni}(\text{oaoH})(\text{oaoH}_2)]\text{tcnq}$ : Temperature dependence of the static magnetic susceptibility.

metal-like properties of the Ni salt are due to some neutral tcnq doped into the tcnq<sup>-</sup> stacks, resulting in a fractional average charge. That some of the tcnq<sup>-</sup> in the solution is oxidized to tcnq<sup>0</sup> during the crystal growth has been observed in the preparation of the Pt compound: Some crystals of neutral tcnq and of the mixed valence phase {[Pt(oaoH)(oaoH<sub>2</sub>)]<sup>+</sup>}<sub>2</sub>[(tcnq)<sub>3</sub>]<sup>2-</sup> could be isolated [16].

From the bond lengths in the tcnq moiety of [Ni(oaoH)(oaoH<sub>2</sub>)]tcnq, a charge of -0.8(1) may be derived [17]. This value seems underestimated, however, as the C≡N stretching frequencies in the ir spectra are typical for fully charged tcnq<sup>-</sup> [18], and are the same as in the Pt salt. So the maximum doping level should be a few per cent.

The observation of a weak resonance Raman band at 1457 cm<sup>-1</sup>, typical for the ν<sub>4</sub> mode of neutral tcnq [19], supports this assumption. However, no ν<sub>4</sub> band attributable to tcnq<sup>-</sup>, expected at 1395 cm<sup>-1</sup>, or to a species with fractional average charge can be detected. The band at 1457 cm<sup>-1</sup> is not observed in the Pt compound, in agreement with its different physical behaviour.

If there is a lack of negative charge on the tcnq<sup>-</sup> stacks, it must be compensated by a lack of positive charge on the metal complex stack. No redox process needs to be involved in this, as a loss of a few per cent of the oxime protons, most likely the disordered

H(6), could compensate the charge. The effect is too small to become evident in the X-ray structure determination. From the difference of the *intermolecular* O—H—O bridges in the Ni and Pt compounds it is understandable, that a loss of the proton involved is energetically less unfavourable in the Ni compound than in the Pt counterpart. So it is easier for the Ni complex stack to be in a "mixed protolytic" state, accompanied by a mixed valence state of the tcnq<sup>-</sup> stack, in accordance with the observed physical properties.

In summary, we have crystallized and characterized the first molecular solid consisting of a metal complex cation and an organic radical anion with metal like properties at room temperature. We have profited from the special properties of the oxamide oxime complexes: capability of extended H bond formation, and tunable positive charge due to the acid-base equilibrium of the oxime groups. Further prospects lie in the synthesis of molecular metals with variable band filling by adjusting the pH during crystallization and using appropriate tcnq/tcnq<sup>-</sup> mixtures.

This work is made possible by a research grant from Stiftung Volkswagenwerk. Financial support from Fonds der Chemischen Industrie and donations of precious metal salts from DEGUSSA, Hanau, are also acknowledged. We thank G. Mair for organizing low temperature X-ray experiments at the MPI für Festkörperforschung, Stuttgart.

- 
- [1] Z. G. Soos and S. R. Bondeson, in J. S. Miller (ed.): "Extended Linear Chain Compounds", Vol. 3, Plenum Press, New York 1983, p. 193.
- [2] W. E. Hatfield (ed.), "Molecular Metals", Plenum Press, New York 1979.
- [3] J. B. Torrance, in Ref. [1], p. 7; *Acc. Chem. Res.* **12**, 79 (1979).
- [4] H. Endres, in Ref. [1], p. 263.
- [5] H. Endres, *Z. Naturforsch.* **37b**, 702 (1982).
- [6] H. Endres, *Angew. Chem.* **94**, 548 (1982), *Angew. Chem. Int. Ed. Engl.* **21**, 524 (1982), *Angew. Chem. Suppl.* **1982**, 1309.
- [7] L. Tschugaeff and J. Surenjanz, *Ber. Dtsch. Chem. Ges.* **40**, 181 (1907); H. Endres and T. Jannack, *Acta Crystallogr.* **B36**, 2136 (1980).
- [8] H. Endres, *Z. Anorg. Allg. Chem.* **513**, 78 (1984).
- [9] P. M. Chaikin and J. F. Kwak, *Rev. Sci. Instrum.* **46**, 218 (1975).
- [10] H. Endres, H. J. Keller, J. Queckbörner, D. Schweitzer, and J. Veigel, *Acta Crystallogr.* **B38**, 2855 (1982).
- [11] H. M. Altschuler, in: M. Sucher and J. Fox (eds): "Handbook of Microwave Measurements", Polytechnic Press, New York and London, 1963.
- [12] G. M. Sheldrick. SHELXTL. An integrated system for solving, refining, and displaying crystal structures from diffraction data. Univ. Göttingen, FRG (1981).
- [13] International Tables for X-ray Crystallography. Vol. IV. Kynoch Press, Birmingham 1974.
- [14] C. S. Jacobsen, K. Mortensen, J. R. Andersen, and K. Bechgaard, *Phys. Rev.* **18**, 905 (1979).
- [15] C. Coulon, P. Delhaes, S. Flandrois, R. Lagnier, E. Bonjour, and J. M. Fabre, *J. Physique* **43**, 1059 (1983).
- [16] H. Endres, *Angew. Chem.* **96**, 993 (1984); *Angew. Chem., Int. Ed. Engl.* **23**, 999 (1984).
- [17] S. Flandrois and D. Chasseau, *Acta Crystallogr.* **B33**, 2744 (1977).
- [18] J. S. Chappell, A. N. Bloch, W. A. Bryden, M. Maxfield, T. O. Poehler, and D. O. Cowan, *J. Am. Chem. Soc.* **103**, 2442 (1981).
- [19] S. Matsuzaki, R. Kuwata, and K. Toyoda, *Solid State Commun.* **33**, 403 (1980).